

# Atlantic watermass and circulation response to persistent freshwater forcing in two coupled general circulation models

M. Harrison · A. Adcroft · R. Hallberg

Received: 1 August 2012/Accepted: 2 May 2013/Published online: 21 May 2013  
© Springer-Verlag (outside the USA) 2013

**Abstract** The sensitivity of the Atlantic circulation and watermasses to biases in the convergence of moisture into the basin is examined in this study using two different general circulation models. For a persistent positive moisture flux into the tropical Atlantic, the average salinity and temperature in the basin is reduced, mainly below mid-depths and in high latitudes. A transient reduction in the Atlantic overturning strength occurs in this case, with a recovery timescale of 1–2 centuries. In contrast, a similar amount of freshwater directed into the Subpolar North Atlantic results in a persistent reduction in overturning and an increase in basin heat and salt content. In the unperturbed pre-industrial simulations, the Atlantic is unambiguously warmer and saltier than historical observations below mid-depths and in the Nordic Seas. The models' tropical freshwater flux sensitivities project strongly onto the spatial pattern of this bias, suggesting a common atmospheric deficiency. The integrated Atlantic plus Arctic surface freshwater flux in these models is between  $-0.5$  and  $-0.6$  Sv, compared with an observational estimate of  $-0.28$  Sv. Our results suggest that shortcomings in the models' ability to reproduce realistic bulk watermass properties are due to an overestimation of the inter-basin moisture export from the tropical Atlantic.

**Keywords** Freshwater fluxes · Atlantic · Climate model bias · CMIP5 · GFDL · AMOC

---

M. Harrison (✉) · R. Hallberg  
NOAA/GFDL, Princeton University Forrestal Campus,  
201 Forrestal Road, Princeton, NJ 08540-6649, USA  
e-mail: matthew.harrison@noaa.gov

A. Adcroft  
Princeton University, Princeton, NJ 08542, USA

## 1 Introduction

The present generation of climate models are routinely run without artificial air-sea flux adjustments for heat and freshwater. The ability of such models to maintain fairly realistic watermass properties near the ocean surface and below is demonstrative of improvements in the representation of relevant processes which have been realized in recent years. Further inroads in coupled model development are predicated on their ability to improve the mean hydrographic state and circulation of the ocean. To this end, it is important to understand the nature, and potential sources, of biases, both in the composition of watermasses as well as in the circulation, as they exist in coupled climate model applications. In this study, we will examine the impact of persistent inter-basin moisture transport anomalies on basin-scale watermass biases and the Atlantic overturning circulation strength in two coupled general circulation models.

Numerous studies have used coupled GCMs to examine the response of the ocean circulation to freshwater input. Manabe and Stouffer (1997), for example, tested their models' sensitivity to a 0.1 Sv flux of freshwater introduced into the North Atlantic deep water (NADW) formation regions over a 500 year period. This perturbation caused surface air temperatures in the North Atlantic to cool, sea ice coverage to extend further South, and the North Atlantic meridional overturning circulation (AMOC) to weaken. The same amount of freshwater applied in the subtropical North Atlantic resulted in a similar evolution of the climate system, however the magnitude of the response was 4–5 times smaller. It is a broadly accepted conclusion from these and other studies (e.g. Weijer et al. 1999; Schmittner and Clement 2002) that freshwater flux anomalies at higher latitudes in the Atlantic basin are more effective at weakening the strength of the AMOC, and that

their impact decreases away from the regions of dense water formation in the North Atlantic. The sensitivity of models to increased freshwater flux in the North Atlantic is usually discussed in the context of calving fluxes from Greenland glaciers (e.g. Broecker 1994; Barber et al. 1999; Weijer et al. 2012). An observational estimate of the present-day rate of Greenland mass discharge is about 30 % of the canonical 0.1 Sv used in so-called “water hosing” experiments (Bamber et al. 2012).

Additionally, there has been speculation that sustained shifts in the distribution of El Niño or La Niña events could influence the formation of NADW. Schmittner et al. (2000) estimated that an additional 0.1 Sv of freshwater are retained in the Atlantic during moderate La Niña events. Spence and Weaver (2008) performed a careful evaluation of the Atlantic overturning response to ENSO-related freshwater forcing. The AMOC was not particularly responsive to typical ENSO forcing in their model, however larger amplitude freshwater transport anomalies on decadal and longer timescales did generate a significant overturning response.

It is evident that non flux-adjusted climate models are prone to persistent freshwater forcing biases. This could contribute to an artificially strong or weak AMOC magnitude in historical and future climate scenarios. Freshwater flux estimates, which have been derived from ocean hydrographic transects, or ocean and/or atmospheric reanalyses (for example, Rienecker et al. 2009; Nicolas and Bromwich 2011), may provide some guidance in the interpretation of climate model results. Talley (2008) (hereafter, T08), for instance, estimate the net freshwater forcing in the combined Atlantic and Arctic basins, between the Bering Strait and 32°S, at  $-0.28 \pm 0.04$  Sv. This result will be used as a basis for comparison with the models described in this manuscript. Our results are generated from two coupled climate models (Dunne et al. 2012). The Atlantic plus Arctic freshwater forcing in these models is between  $-0.5$  and  $-0.6$  Sv, a bias which exceeds the annual mean discharge from the Amazon river.

The two models presented in this study share common ocean surface freshwater flux and subsurface biases, i.e. an Atlantic basin which is overly evaporative, salty and warm (relative to the global average temperature). We will introduce a persistent positive freshwater flux anomaly into the Atlantic basin, balanced by an equal and opposite evaporative flux in the Western Tropical Pacific. The resulting perturbed ocean state will be evaluated in light of the biases in the unperturbed pre-industrial control simulations.

## 2 Observations

The observational datasets used here are: precipitation over land and ocean, GPCP (Adler et al. 2003); column-

integrated heat and salt content from the 2009 NODC World Ocean Atlas, WOA09 (Locarnini et al. 2010; Antonov et al. 2010); freshwater transports derived from high-density ocean transects (T08); and an inversion estimate of the AMOC, based on air-sea fluxes, hydrographic sections and direct current measurements (Lumpkin and Speer 2007).

The GPCP combined precipitation data were developed and computed by the NASA/Goddard Space Flight Center’s Laboratory for Atmospheres as a contribution to the GEWEX Global Precipitation Climatology Project. GPCP precipitation data are based on satellite and gauge measurements from 1979 to 2011.

The WOA09 dataset is considerably warmer than previous analyses from NODC, for example, global average temperatures are approximately 0.2 °C warmer compared to the 1998 version of the atlas. This may be attributable to changes in the observing system as well as natural and/or anthropogenic effects. For our analysis, the global average heat content bias was subtracted from the model results in order to compensate for temperature drift over the course of the runs. Global salt content is nearly identical between the models and observations, since the models were initialized with NODC data, therefore no adjustments were necessary for this quantity. We performed our analysis using the 1998 version of the NODC Atlas in addition to WOA09 and our results were not impacted significantly.

The freshwater transports in T08 were calculated from absolute geostrophic velocities and Ekman transports. Absolute geostrophic velocity estimates from Reid (1997) were used along with NCEP Reanalysis winds (1979–2005) for the Ekman transport with integral adjustments based on a Bering Strait transport estimate of 1 Sv. Bering Strait transport is subject to considerable variability on seasonal to inter-annual timescales with a range exceeding  $\pm 1$  Sv (Woodgate et al. 2006). T08, however, found negligible sensitivity of Atlantic freshwater transport to the prescribed Bering Strait freshwater transport in her calculation. The Ekman component of the freshwater transport was calculated using climatological salinity at 30 m and the absolute geostrophic salinity transport uses CTD profiles and bottle data interpolated at 10 dbar intervals. Her estimate of oceanic freshwater import is  $0.28 \pm 0.04$  Sv measured between Bering Strait and 32°S and roughly 0.6 Sv South of 45°N. These estimates are roughly consistent with previous hydrographic estimates from Ganachaud and Wunsch (2003) and air-sea flux estimates from Wijffels et al. (1992).

The AMOC is not directly observable and its magnitude is estimated using some combination of direct current measurements, hydrographic sections and winds. For example, Cunningham et al. (2007) measured the overturning at 26.5°N and calculated a year-long average of

$18.7 \pm 5.6$  Sv. Lumpkin and Speer (2007) arrived at estimates of the overturning circulation, by divided the ocean into 45 neutral density layers and integrating the surface heat and freshwater fluxes between density outcrops, incorporating parameterizations for advective and mixing processes in the interior. Five different surface flux products were used to arrive at a mean surface transformation rate. The interior fluxes were constrained using hydrographic sections from the World Ocean circulation experiment (WOCE) with additional constraints for mass, heat, salt and top-to-bottom integrated silicate. Their estimate of the maximum overturning at  $48^{\circ}\text{N}$  in the Atlantic is  $16.3 \pm 2.7$  Sv.

### 3 Coupled model description

The coupled models are based on the earth system models (ESMs) documented by Dunne et al. (2012). The atmospheric grid is  $2.5^{\circ} \times 2^{\circ}$  with 24 vertical levels. The atmosphere, land, sea–ice and ocean models conservatively exchange heat, freshwater, tracers and momentum every 2 h. The ocean models use independent dynamical/physical cores: CM2M (Griffies et al. 2005) is the designation given to the coupled model with a  $z^*$  vertical coordinate; CM2G uses an ocean model with an isopycnal vertical coordinate (Hallberg and Adcroft 2009) coupled to a bulk mixed layer at the surface. Both models use  $1^{\circ}$  nominal horizontal resolutions, with 50 (CM2M) and 63 (CM2G) vertical levels or layers. Both CM2M and CM2G exchange freshwater with the atmosphere and land component models as opposed to virtual salt fluxes. The initial conditions for both CM2M and CM2G were taken after more than 1,000 model years of integration of the ESM2M and ESM2G runs with year 1860 solar and radiative forcing, corresponding to the initial states used for the twentieth century simulations submitted to the coupled model intercomparison project (CMIP5). All of the sensitivity experiments presented here were integrated for an additional 1,000 model years from these initial conditions using 1860 solar and radiative forcings. The models whose sensitivities are presented in this manuscript are configured identically to the pre-industrial runs with the ecosystem model disabled. The decision to remove the biological component was made for computational reasons. In place of the internally generated phytoplankton from the ESMs, we used prescribed ocean chlorophyll (Anderson et al. 2009).

### 4 Model freshwater forcing and hydrographic biases

After a multi-centennial spinup using pre-industrial radiative forcings, the ESMs described in Dunne et al. (2012)

were integrated with time-varying radiative gas concentrations and solar forcing for the historical period from 1861 to 2005. We begin this section with a description of the precipitation and sea surface salinity (SSS) biases in both ESMs for the historical period. Large biases were identified in the Western tropical Pacific, where precipitation is excessive and SSS is overly fresh, and in the Amazon basin, where conditions are dry and salty water accumulates near the mouth of a weakened Amazon river. The surface freshwater biases were nearly identical in both models runs with 1860 radiative forcings and in the CM2 experiments (not shown). We follow with a description of the interior biases in the CM2 runs and document the presence of a warm and salty bias in the Atlantic basin in both models (after adjusting for global temperature drifts). The presence of these biases motivated the design of the sensitivity experiments described in Sect. 5.

#### 4.1 GFDL/CMIP5 ESM's precipitation and surface salinity bias

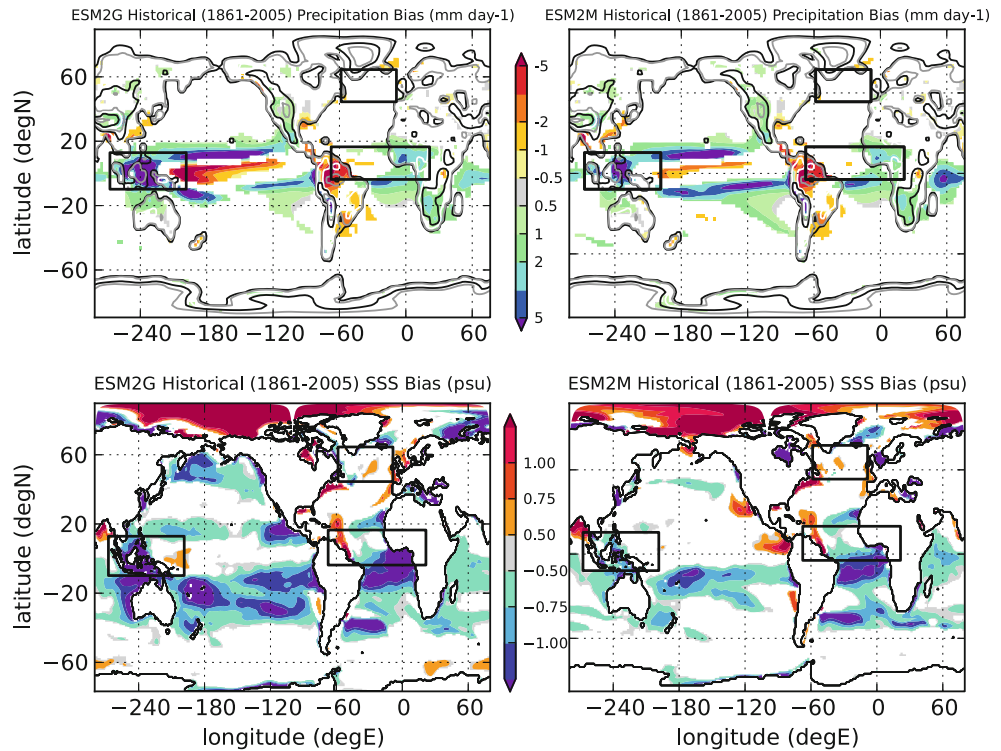
The top panels of Fig. 1 show the time mean precipitation differences from GPCP for the ESM2M and ESM2G historical runs (1861–2005). Both ESM2M and ESM2G (and CM2M and CM2G) exhibit qualitatively similar biases in precipitation and SSS. The pattern of tropical rainfall bias in both models is typical of the CMIP4 suite (Dai 2006), including the closely related CM2.1 model (Delworth et al. 2006).

Both models exhibit a double-ITCZ bias in the Pacific and a Southward shift in the Atlantic ITCZ. They also have a consistent pattern of excessive rainfall in the Western tropical Pacific around Indonesia and dry conditions in the Amazon basin. The atmospheric model orography is subject to significant smoothing (for numerical reasons). The contours over land in the top panel of Fig. 1 indicate the elevations used by the model; of particular interest, the average height over the Andean plateau is 1–2 km, compared to about 4 km in reality.

The precipitation biases in the tropical West Pacific are larger in ESM2G compared to ESM2M. The magnitude of the rainfall bias over the Amazon is similar in both models and is underestimated by 0.1–0.15 Sv, based on comparisons to runoff estimates (Dai and Trenberth 2002). Conditions over most of Sub-Saharan Africa and the Western Tropical Indian ocean are too wet in both models; South-Eastern South America and the Northern Bay of Bengal are too dry, likewise in both models. The pattern of the rainfall biases are reflected, not surprisingly, in the patterns of the surface salinity bias.

The bottom panels in Fig. 1 show the SSS bias. The SSS biases are well correlated with the precipitation biases over large portions of the tropics. For example: the dry-salty

**Fig. 1** GFDL/CMIP5 ESM historical run annual precipitation bias (*top panels*) and surface salinity bias (*bottom panels*) from model years 1861–2005 compared with GPCP and WOA09 respectively. Precipitation biases are masked where the absolute value is less than the standard error of the GPCP data. Salinity biases are masked for absolute values <0.4 PSU. The left side of the figure is ESM2G bias and the right hand side is ESM2M bias. The boxes show the regions for which the precipitation is altered in the sensitivity studies. The contours over land in the *top panels* indicate the model orography (CI = 50, 100, 500, 1,000, 2,000, 3,000 and 4,000 m)



surface bias near the Amazon and at points downstream to the North; the wet-fresh bias in the South Pacific convergence zone (SPCZ) and around Indonesia as well as in the Congo basin; and the dry salty bias in the Northern Bay of Bengal, exist in both models. ESM2G has larger biases in both precipitation and surface salinity throughout much of the tropics. Partly, this reflects differences in the effective minimum mixed layer depths, a 2 m minimum in ESM2M and a 10 m minimum in ESM2G, which can lead to large differences in SSS with locally strong freshwater forcing. Outside of the tropics, the correspondence between SSS and precipitation bias is not nearly as evident, suggesting a more prominent role for the ocean circulation and much deeper mixed layers seasonally. Both models exhibit a large salty surface bias throughout the Arctic Basin due to a poor representation of the surface halocline in this region.

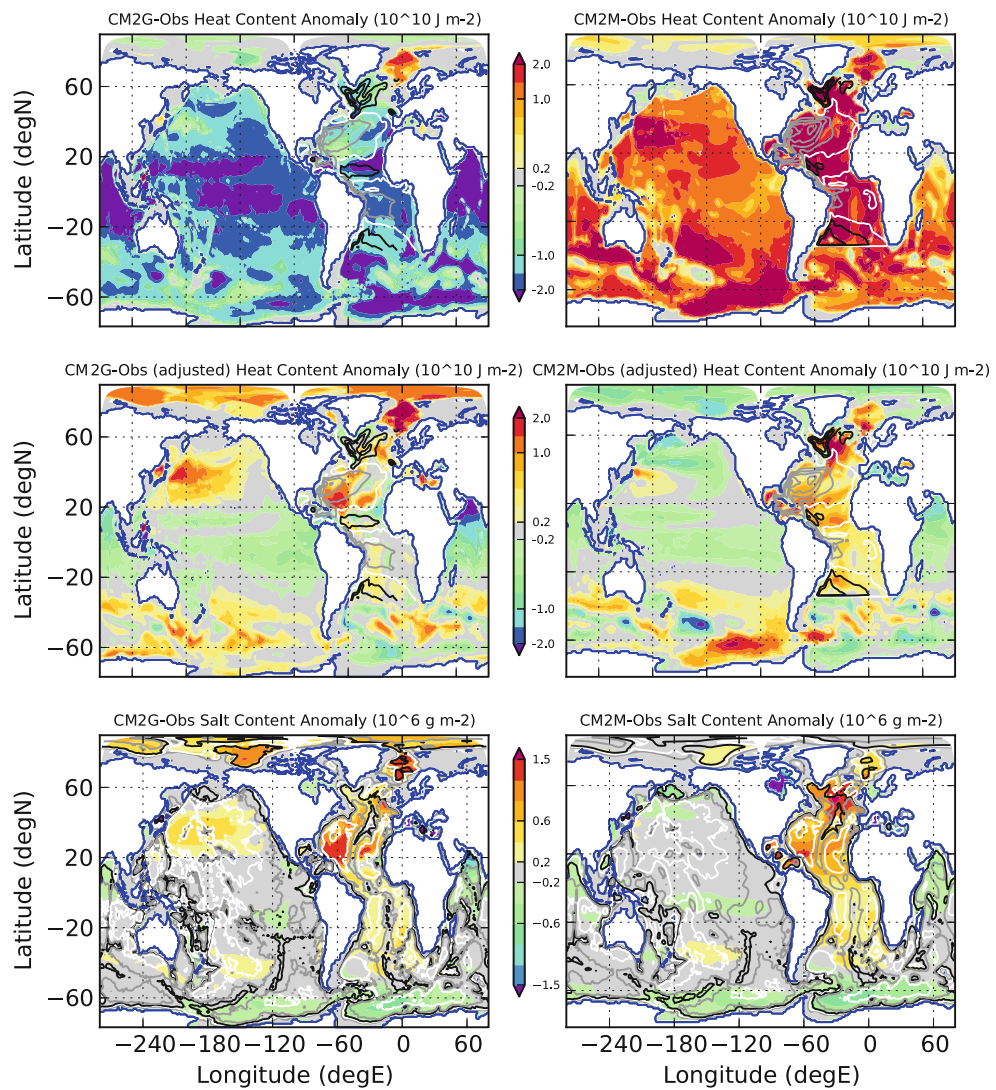
#### 4.2 CM2M and CM2G interior biases

Turning to the ocean interior, Fig. 2 shows the column-integrated heat and salt bias in our CM2M and CM2G experiments (averaged from years 750–1,000) compared to WOA09. CM2M is significantly warmer than observations while in contrast, CM2G is cooler. The top of atmosphere radiative imbalance is  $<0.25 \text{ W m}^{-2}$  in both models at this stage in the pre-industrial spinup, indicating that the models are roughly in thermal equilibrium. CM2M is significantly warmer than observations due to a larger positive radiative imbalance during earlier stages of the spinup

(conversely for CM2G). The differences in the ocean heat content in CM2G and CM2M are due entirely to differences in the ocean model formulation. The excess heat in CM2M is stored mostly below the upper few hundred meters, with globally-averaged values ranging from 1 °C near 500 m up to about 1.5 °C in the abyss. The globally-averaged cold bias in CM2G attains a peak value of  $-1.5$  °C near 1 km and decreases with depth; CM2G global bias below 2.5 km is  $<0.1$  °C.

In order to compare the spatial distribution of heat storage between models and observations, we eliminated the global mean bias in the middle panels of Fig. 2. In the lower panels, the bias in the salt content is shown for both models, for which no adjustment is necessary because the models were initialized with WOA data and salt is roughly conserved within the ocean. Contours of the horizontal gyre circulation are shown on top of the heat content panels and model bathymetry is contoured above the salinity panels. The excess heat and salt in the Atlantic is most strongly aligned with the bathymetry, indicative of the fact that the model biases are largely below the mid-Atlantic ridge, and below the level of surface-intensified gyres. Errors associated with vertical displacements of isopycnal surfaces are dominant within the thermocline while mid-depth and deep biases are largely associated with density-compensated watermass biases within weakly stratified isopycnal layers. Below mid-depths, watermasses are almost uniformly too warm and salty in the Atlantic.

**Fig. 2** Control run depth-integrated heat (*top* and *middle*,  $10^{10} \text{ J m}^{-2}$ ) and salt (*bottom*,  $10^6 \text{ g m}^{-2}$ ) biases for CM2G (left) and CM2M (right) averaged from years 750 to 1,000 of the simulation. The *top panel* shows the heat content biases prior to subtracting the global warming (CM2M) or cooling (CM2G) signal in the models. The adjusted heat content is shown in the *middle panels*. In the *top two panels*, black (counter clockwise) and grey (clockwise) contours are the Atlantic ocean gyre circulation in 10 Sv intervals. In the *bottom panel*, the ocean bathymetry is contoured at 1,000 m intervals



## 5 Sensitivity experiments

Figure 3 shows the net freshwater forcing in both models for the control and perturbation experiments described below. The integrated forcing in the combined Atlantic and Arctic basins (North of  $30^\circ\text{S}$ ) is shown in the top panels. The middle panels show the net forcing in the tropical Atlantic from  $5^\circ\text{S}$  to  $20^\circ\text{N}$  and the lower panels are the time-series integrated North of  $45^\circ\text{N}$ .

Both models are net evaporative in the combined Atlantic and Arctic basins, with CM2G exporting about 0.57 Sv and CM2M exporting roughly 0.54 Sv of freshwater (averaged over years 750–1,000) compared to the 0.28 Sv estimate from T08. For the latitude range from  $30^\circ\text{S}$  to  $45^\circ\text{N}$ , she estimates 0.59 Sv of freshwater export. For roughly the same range of latitudes, both CM2G and CM2M have a net forcing of approximately 0.9 Sv (taking the difference between the top and bottom panels in Fig. 3). CM2M receives about 0.05 Sv more precipitation North of  $45^\circ\text{N}$  relative to CM2G.

In our experiments, we extracted a fraction of the rainfall over the Indonesian region and precipitated this same amount over the Atlantic in the regions indicated by the rectangles in Fig. 1. The global net freshwater forcing perturbation is zero, so this adjustment is akin to a shift in the hydrological cycle rather than a release of freshwater from glaciers. In our sensitivity tests, 20 % of the net precipitation received in the Tropical West Pacific region was uniformly distributed in the Atlantic in either the tropical region from  $5^\circ\text{S}$  to  $15^\circ\text{N}$  (FwEq) or the Northern subpolar gyre from  $45^\circ\text{N}$  to  $65^\circ\text{N}$  (FwNA). The precipitation anomalies were continued over the course of the 1,000 year integrations.

The red lines indicate the freshwater flux in the respective regions in FwEq-G and FwEq-M. The magnitude of the inter-basin moisture transport anomaly is approximately 0.2 Sv in FwEq-G and 0.1 Sv in FwEq-M (precipitation is more intense around Indonesia in CM2G). The figures show that the freshwater balance in the FwEq

**Fig. 3** Net freshwater forcing in CM2G (left) and CM2M-based models (right). Top Atlantic plus Arctic basins North of 30°S, middle Atlantic basin from 5°S to 20°N, bottom Atlantic plus Arctic basins North of 45°N. CM2G and CM2M (black), FwEq-G and FwEq-M (red), FwNA-G and FwNA-M (blue). Units are  $Sv \equiv 10^6 m^3 s^{-1}$

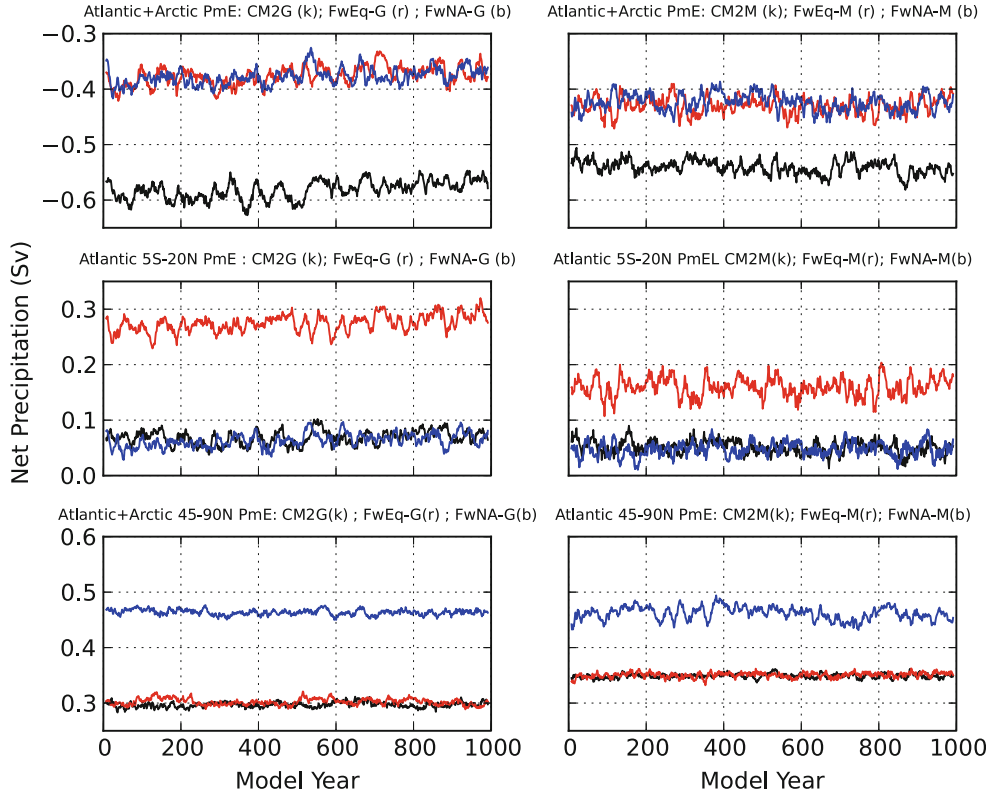
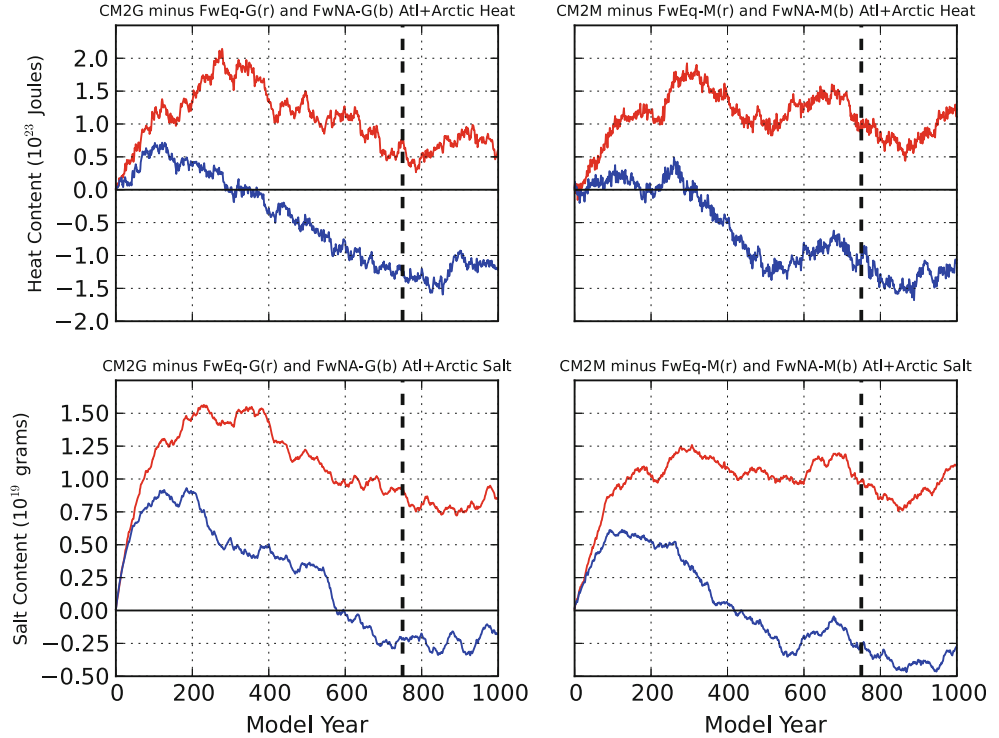


**Fig. 4** FwEq (r) and FwNA (b) Atlantic + Arctic heat and salt content differences from respective CM2G (left) and CM2M (right) control simulations. Our analysis is based on the time-average quantities for model years 750–1,000



experiments was not impacted outside of the tropical Atlantic where the adjustment was applied and that the perturbation was fairly steady throughout the experiment.

The FwNA experiments are indicated by the blue lines. Again, the magnitude of the freshwater anomaly was about 50 % smaller in the FwNA-M experiment compared to

**Table 1** Heat, salt, AMOC and freshwater forcing bias in our experiments: Atlantic (South of 65°N) and Arctic heat and salt content bias for the CM2G and CM2M control runs and for the corresponding FwEq and FwNA experiments ( $10^{23}$  J and  $10^{19}$  gsalt);

|  | CM2G      | FwEq–G     | FwNA–G      |
|--|-----------|------------|-------------|
| Atl heat bias (% reduction)                  | 0.73 (–)  | 0.15 (73)  | 2.10 (–190) |
| Arctic heat bias (% reduction)               | 0.68 (–)  | 0.60 (11)  | 0.55 (19)   |
| Atl + Arctic heat bias (% reduction)         | 1.41 (–)  | 0.75 (47)  | 2.66 (–89)  |
| Atl salt bias (% reduction)                  | 1.85 (–)  | 1.14 (38)  | 2.24 (–21)  |
| Arctic salt bias (% reduction)               | 0.33 (–)  | 0.23 (30)  | 0.17 (48)   |
| Atl + Arctic salt bias (% reduction)         | 2.18 (–)  | 1.37 (37)  | 2.41 (–11)  |
| Atl FW flux bias South of 40°N (% reduction) | –0.30 (–) | –0.10 (67) | –0.30 (0)   |
| Atl + Arctic FW flux bias (% reduction)      | –0.29 (–) | –0.09 (69) | –0.09 (69)  |
| AMOC 40–45°N bias                            | 2.1       | 1.9        | –0.4        |
|  | CM2M      | FwEq–M     | FwNA–M      |
| Atl heat bias (% reduction)                  | 3.63 (–)  | 2.78 (23)  | 4.96 (–37)  |
| Arctic heat bias (% reduction)               | –0.31 (–) | –0.32 (–3) | –0.34 (–10) |
| Atl + Arctic heat bias (% reduction)         | 3.32 (–)  | 2.45 (26)  | 4.63 (–39)  |
| Atl salt bias (% reduction)                  | 3.21 (–)  | 2.38 (26)  | 3.74 (–16)  |
| Arctic salt bias (% reduction)               | 0.12 (–)  | 0.04 (67)  | –0.03 (75)  |
| Atl + Arctic salt bias (% reduction)         | 3.33 (–)  | 2.42 (27)  | 3.71 (–11)  |
| Atl FW flux bias South of 40°N (% reduction) | –0.33 (–) | –0.21 (36) | –0.32 (3)   |
| Atl + Arctic FW flux bias (% reduction)      | –0.27 (–) | –0.15 (44) | –0.15 (44)  |
| AMOC 40–45°N bias                            | 8.9       | 7.9        | 5.1         |

FwNA–G. Likewise, the integrated freshwater balance in both FwNA experiments was not impacted outside of the region over which the anomalous flux was applied.

The FwEq and FwNA sensitivity experiments were integrated for 1,000 years. The time-series of combined Atlantic and Arctic heat and salt content anomalies are shown in Fig. 4. For the analysis which follows, the time averages are computed over model years 750–1,000. Table 1 summarizes our sensitivity results.

### 5.1 Model sensitivity to tropical Atlantic freshwater

Figure 5 shows the depth-integrated CM2 minus FwEq (globally adjusted) heat and salt content anomalies. The horizontal gyres in CM2G and CM2M are contoured in the upper panels and the gyre anomalies are contoured in the lower panels. The freshwater flux anomalies have a negligible impact on the gyre circulation in both models. On the other hand, it leaves an indelible imprint on interior watermasses. The globally adjusted heat and salt content biases for the FwEq runs are summarized in Table 1 for the combined Atlantic and Arctic (separated at 65°N) and for the two basins separately.

The Atlantic heat bias was reduced by 73 and 23 % and the salt bias decreased 38 and 26 % in FwEq–G and FwEq–M, respectively. The correlation between FwEq heat

freshwater forcing bias between 30°S and 40°N and between Bering Strait and 30°S (Sv); and the AMOC index bias (Sv) calculated between 40 and 45°N for the model experiments and at 48°N in Lumpkin and Speer (2007)

anomalies in the Atlantic and the control biases were 0.43 and 0.44, respectively. Atlantic salinity anomaly correlations with the control bias were larger at 0.78 and 0.77 for FwEq–G and FwEq–M.

In the Arctic, the heat and salt biases reduced by 11 and 30 % respectively in FwEq–G and bias correlations were 0.56 and 0.88. In FwEq–M, the Arctic heat content sensitivity was comparatively weak, while the salt bias decreased by 67 % and the anomaly correlation was 0.57. We note that the watermass biases in the Arctic were substantially smaller in CM2M relative to CM2G and this may be attributable to the additional Arctic precipitation in CM2M.

Figure 6 shows the AMOC time-series in the North Atlantic between 40–45°N (the index was based on the maximum overturning in density coordinates between these latitudes). A transient reduction of the AMOC occurred in both models, lasting for about two centuries, after which the overturning anomalies became smaller.

The AMOC reduction averaged over the first 200 years was 3.9 and 1.0 Sv, corresponding to a transient overturning sensitivity of about 9 and 4 % in FwEq–G and FwEq–M, respectively, for a 0.1 Sv perturbation in the tropical freshwater flux. The time-average AMOC index during years 750–1,000 was reduced by 1 and 4 % between years 750 and 1,000 from 18.4 and 25.2 Sv in FwEq–G and

**Fig. 5** CM2G and CM2M minus FwEq-G and FwEq-M depth-integrated temperature and salinity anomalies. The contours in the top panels show the CM2G and CM2M Atlantic gyre streamfunction in 10 Sv intervals (gray clockwise, black counter-clockwise). The bottom panel contours are the anomalous Atlantic gyre streamfunction anomalies in 2 Sv intervals. Differences shown are averages from years 750–1,000

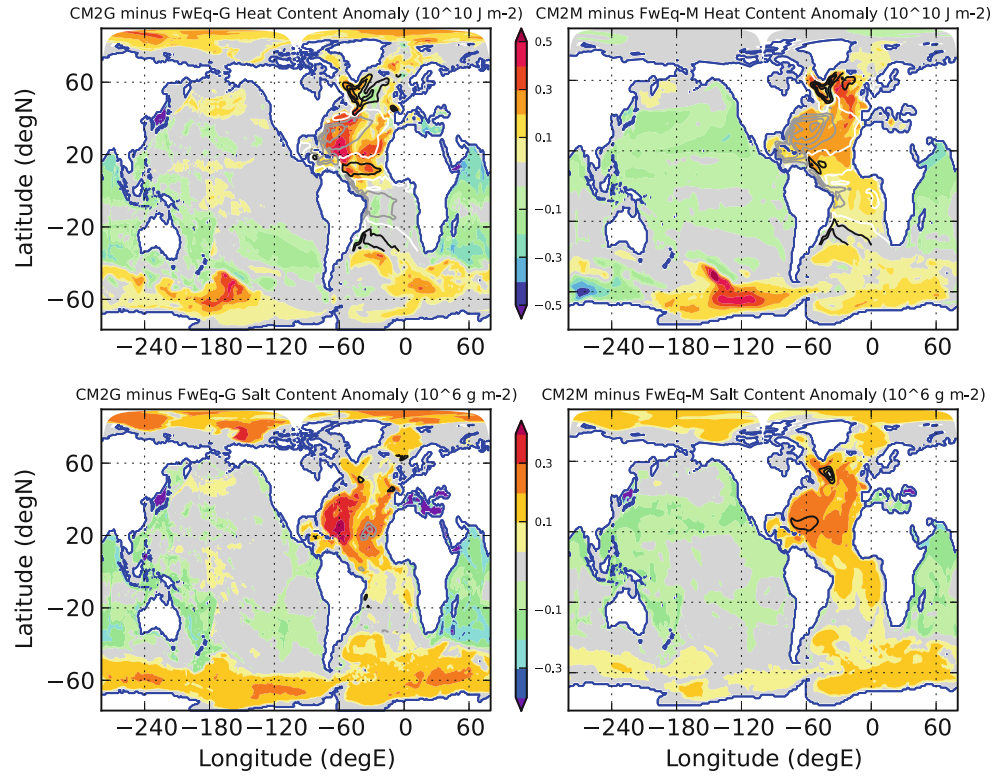
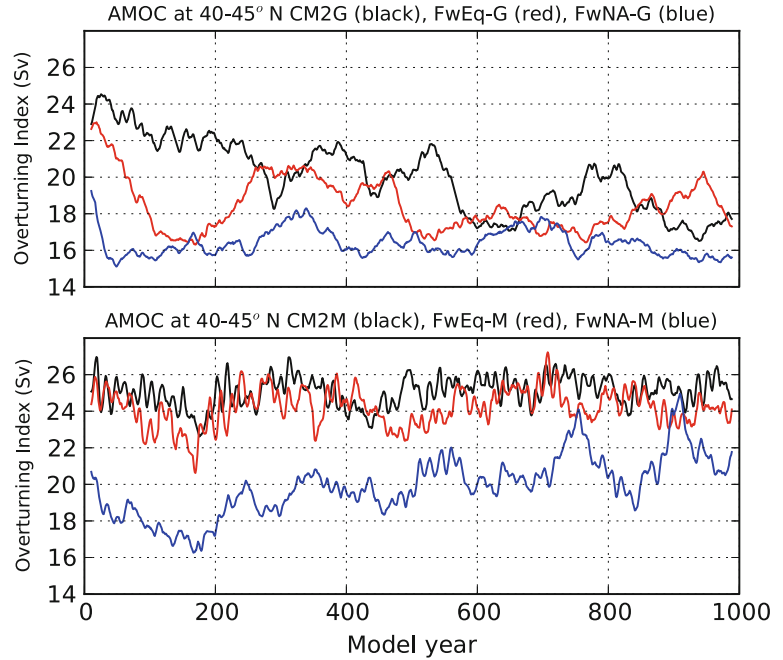


**Fig. 6** AMOC measured between  $40^{\circ}\text{N}$  and  $45^{\circ}\text{N}$  for CM2G and its perturbation experiments (top) and the CM2M runs (bottom): CM2G and CM2M (black), FwEq (red), FwNA (blue). Units are Sv. A 20 year running mean was applied to the AMOC time-series

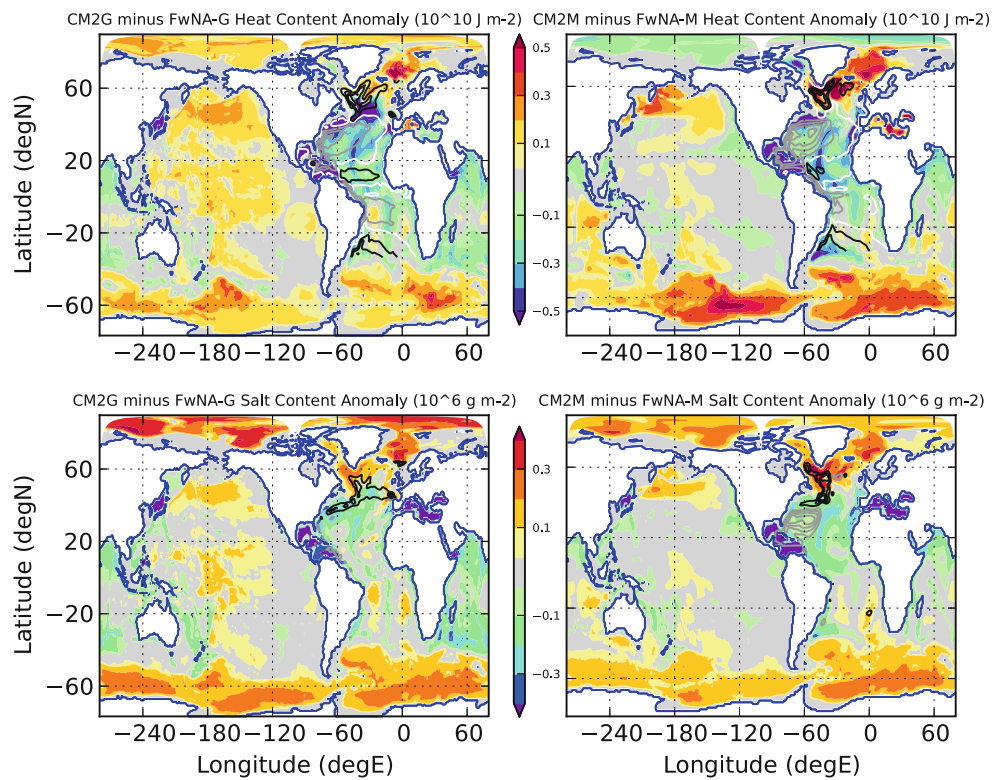


FwEq-M respectively. Lumpkin and Speer (2007) estimate an overturning magnitude of  $16.3 \pm 2.7$  Sv at these same latitudes. CM2G and FwEq-G are therefore within the range of observational uncertainty while CM2M and FwEq-M appear to overestimate the AMOC strength.

In summary, the AMOC exhibited a larger transient reduction in FwEq-G compared to FwEq-M and was

marginally impacted on longer timescales in both experiments. The approximate 0.2 Sv freshwater adjustment applied in experiment FwEq-G yielded a 47 % reduction in Atlantic plus Arctic heat content bias and a salt bias reduction of 37 % relative to CM2G. For FwEq-M, the roughly 0.1 Sv perturbation resulted in a 26 % decrease in heat content bias and a 27 % reduction in salt bias for the

**Fig. 7** Same as Fig. 5, but for CM2G and CM2M minus FwNA-G and FwNA-M respectively



combined basins. The freshwater flux anomaly in the FwEq experiments corresponds to a 67 and 44 % bias reduction measured between Bering Strait and 30°S for CM2G and CM2M respectively.

The next section examines the models' sensitivity to an identical freshwater flux anomaly applied within the North Atlantic subpolar gyre.

## 5.2 Model sensitivity to North Atlantic freshwater

Consistent with previous studies, the models' AMOC was more responsive to freshwater forcing at higher latitudes. In FwNA-G and FwNA-M, the reduction in AMOC was sustained over the course of the 1,000 year experiments (Fig. 6, blue lines). The year 750–1,000 average AMOC decreases by 2.4 and 3.7 Sv in FwNA-G and FwNA-M (13 and 14 %) for their respective flux anomalies of 0.2 and 0.1 Sv, corresponding to a 7 and 14 % AMOC sensitivity, respectively, for a 0.1 Sv anomaly.

Figure 7 shows the column-integrated temperature, salinity and gyre response in the FwNA experiments. Both FwNA-M and FwNA-G exhibited a robust circulation and watermass response to subpolar precipitation anomalies and the interior biases are generally degraded in both models (compare to Fig. 2). Consistent with the AMOC reduction, the subpolar gyre strength weakened by roughly 4 Sv (13 %) and 6 Sv (20 %) in FwNA-G and FwNA-M, respectively.

The approximate 0.2 Sv freshwater adjustment applied in experiment FwNA-G yielded an 89 % increase in Atlantic plus Arctic heat content bias and a salt bias increase of 11 % relative to CM2G. The Atlantic basin heat and salt biases increased by 190 and 21 % respectively. Conversely, the Arctic biases in the FwNA-G case decreased by 19 and 48 % with bias anomaly correlations of 0.71 and 0.88 for heat and salt. The 0.1 Sv freshwater flux in FwNA-M resulted in a 39 % increase in heat content bias and a 11 % increase in salt bias for the combined Atlantic and Arctic basins.

## 6 Concluding remarks

In CM2G and CM2M, the combined Atlantic and Arctic basins are evaporative at a rate of 0.5–0.6 Sv. The best estimate from T08 is 0.28 Sv. Her estimate in the Atlantic, South of 45°N, is 0.59 Sv, compared to the model results of approximately 0.9 Sv. Thus, a roughly 0.3 Sv moisture transport bias is postulated to exist mostly South of 45°N in both models. The Arctic basin received about 0.07 Sv more precipitation in CM2M compared to CM2G.

Integrated temperature and salinity biases are qualitatively similar in both CM2 models. The Atlantic basin is too salty and too warm, relative to the global average, and this is suggestive of a common atmospheric deficiency. As a sensitivity test, we perturbed the freshwater balance in

the tropical Atlantic, between 5°S and 15°N (FwEq), or into the subpolar Atlantic between 45°N and 65°N (FwNA). We have demonstrated a significant reduction in the ocean interior bias in our FwEq experiments. Conversely, the FwNA experiments resulted in an increase in Atlantic bias in both models. CM2M appears to have about twice the equilibrium freshwater forcing sensitivity as CM2G. In all of the CM2G experiments, the AMOC magnitude is within the range of uncertainty reported by Lumpkin and Speer (2007). The AMOC in CM2M is overestimated in all cases.

In summary, we have provided evidence that these CMIP5 models overestimate the moisture export from the tropical Atlantic to the Pacific and that this bias is strongly correlated with interior oceanic biases. The freshwater forcing in the Atlantic and Arctic basins is an important factor in the stability of AMOC to climatic perturbations (e.g. Huisman et al. 2010; Sijp 2012). Reducing freshwater flux biases for historical simulations would therefore lend greater credibility to future climate model projections.

**Acknowledgments** M. Harrison is grateful to Rym Msadek and Rong Zhang for their feedback on an earlier version of this manuscript. Also, thanks to Robbie Toggweiler for several useful discussions. Two anonymous reviewers provided exceptional reviews and we are thankful for their efforts. All of the analysis and figures presented here were programmed exclusively in Python using freely-available packages including Numpy, Matplotlib, and NetCDF-4.

## References

- Adler R, Huffman G, Chang A, Ferraro R, Xie S, Janowiak J, Rudolf B, Schneider U, Curtis S, Bolvin D, Gruber A, Susskind J, Arkin P, Nelkin E (2003) The version-2 global precipitation climatology project (GPCP) monthly precipitation analysis (1979–present). *J Hydrometeorol* 4:1147–1167
- Anderson WG, Gnanadesikan A, Wittenberg AT (2009) Regional impacts of ocean color on tropical pacific variability. *Ocean Sci* 5(3):313–327
- Antonov JI, Seidov D, Boyer TP, Locarnini RA, Mishonov AV, Garcia HE, Baranova O, K Zweng MM, Johnson DR (2010) World Ocean Atlas 2009, vol 2: salinity. In: Levitus S (ed) NOAA Atlas NESDIS 68. US Government Printing Office, Washington, DC p 184
- Bamber J, van den Broeke M, Ettema J, Lenaerts J, Rignot E (2012) Recent large increases in freshwater fluxes from greenland into the North Atlantic. *Geophys Res Lett* 39(19):L19501
- Barber D, Dyke A, Hillaire-Marcel C, Jennings A, Andrews J (1999) Forcing of the cold event of 8,200 years ago by catastrophic drainage of laurentide lakes. *Nature* 400:344–348
- Broecker W (1994) Massive iceberg discharges as triggers for global climate change. *Nature* 372:421–424
- Cunningham S, Kanzow T, Rayner D, Baringer M, Johns W, Marotzke J, Longworth H, Grant E, Hirschi J, Beal L, Meinen C, Bryden H (2007) Temporal variability of the Atlantic meridional overturning circulation at 26.5°N. *Science* 317:935–938
- Dai A (2006) Precipitation characteristics in eighteen coupled climate models. *J Clim* 19:4605–4630
- Dai A, Trenberth K (2002) Estimates of freshwater discharge from continents: latitudinal and seasonal variations. *J Hydrometeorol* 3:660–687
- Delworth TL et al (2006) GFDL's CM2 global coupled climate models. Part I: formulation and simulation characteristics. *J Clim* 19:643–674
- Dunne J et al (2012) GFDLs ESM2 global coupled climate-carbon earth system models. Part I: physical formaulation and baseline simulation characteristics. *J Clim* 25:6646–6666
- Ganachaud A, Wunsch C (2003) Large-scale ocean heat and freshwater transports during the world ocean circulation experiment. *J Clim* 16:696–705
- Griffies SM et al (2005) Formulation of an ocean model for global climate simulations. *Ocean Sci* 1:45–79
- Hallberg R, Adcroft A (2009) Reconciling estimates of the free surface height in lagrangian vertical coordinate ocean models with mode-split time stepping. *Ocean Model* 29(1):15–26
- Huisman S, den Toom M, Dijkstra HA (2010) An indicator of the multiple equilibria regime of the Atlantic meridional overturning circulation. *J Phys Oceanogr* 40:551–567
- Locarnini RA, Mishonov AV, Antonov JI, Boyer TP, Garcia HE, Baranova OK, Zweng MM, Johnson DR (2010) World Ocean Atlas 2009, vol 1: temperature. In: Levitus S (ed) NOAA Atlas NESDIS 68. US Government Printing Office, Washington, DC, p 184
- Lumpkin R, Speer K (2007) Global ocean meridional overturning. *J Phys Oceanogr* 37:2550–2562
- Manabe S, Stouffer RJ (1997) Coupled ocean-atmosphere model response to freshwater input: comparison to younger dryas event. *Paleoceanography* 12(2):321–336
- Nicolas JP, Bromwich DH (2011) Precipitation changes in high Southern latitudes from global reanalyses: a cautionary tale. *Surv Geophys* 32(4–5):475–494
- Reid JL (1997) On the total geostrophic circulation of the North Atlantic ocean: flow patterns, tracers and transports. *Progr Oceanogr* 39:263–352
- Rienecker M et al (2009) Synthesis and assimilation systems: essential adjuncts to the global observing system, vol 1. In: Ocean obs '09: sustained ocean observations and information for society, p 31
- Schmittner A, Clement AC (2002) Sensitivity of the thermohaline circulaton to tropical and high latitude freshwater forcing during the last glacial-interglacial cycle. *Paleoceanography* 21(2):1–13
- Schmittner A, Appenzeller C, Stocker T (2000) Enhanced Atlantic freshwater export during El Niño. *Geophys Res Lett* 27(8):1163–1166
- Sijp WP (2012) Characterising meridional overturning bistability using a minimal set of state variables. *Clim Dyn* 39:2127–2142
- Spence JP, Weaver AJ (2008) The impact of tropical Atlantic freshwater fluxes ion the North Atlantic meridional overturning circulation. *J Clim* 19:4592–4604
- Talley DL (2008) Freshwater transport estimates and the global overturning circulation: shallow, deep and throughflow components. *Progr Oceanogr* 78(4):257–303
- Weijer W, de Ruijter WPM, Dijkstra HA, van Leeuwen PJ (1999) Impact of interbasin exchange on the Atlantic overturning circulation. *J Phys Oceanogr* 29(9):2266–2284
- Weijer W, Maltrud ME, Hecht MW, Dijkstra HA, Kliphus MA (2012) Response of the Atlantic ocean circulation to greenland ice sheet melting in a strongly-eddyng ocean model. *Geophys Res Lett* 39(9):6
- Wijffels SE, Schmitt R, Bryden H, Stigebrandt A (1992) Transport of freshwater by the oceans. *J Phys Oceanogr* 22:155–162
- Woodgate R, Aagaard K, Weingartner T (2006) Interannual changes in the bering strait fluses of volume, heat and freshwater between 1991 and 2004. *Geophys Res Lett* 33(15):L15609